Organic thin-film transistors: A review of recent advances

by C. D. Dimitrakopoulos
D. J. Mascaro

In this paper we review recent progress in materials, fabrication processes, device designs, and applications related to organic thin-film transistors (OTFTs), with an emphasis on papers published during the last three years. Some earlier papers that played an important role in shaping the OTFT field are included, and a number of previously published review papers that cover that early period more completely are referenced. We also review in more detail related work that originated at IBM during the last four years and has led to the fabrication of high-performance organic transistors on flexible, transparent plastic substrates requiring low operating voltages.

Introduction

For more than a decade now, organic thin-film transistors (OTFTs) based on conjugated polymers, oligomers, or other molecules have been envisioned as a viable alternative to more traditional, mainstream thin-film transistors (TFTs) based on inorganic materials. Because of the relatively low mobility of the organic semiconductor layers, OTFTs cannot rival the performance of field-effect transistors based on single-crystalline inorganic semiconductors, such as Si and Ge, which have charge carrier mobilities (μ) about three orders of magnitude higher [1]. Consequently, OTFTs are not suitable for use in applications requiring very high switching speeds. However, the processing characteristics and demonstrated performance of OTFTs suggest that they can be competitive for existing or novel thin-film-transistor applications requiring large-area coverage, structural flexibility, low-temperature processing, and, especially, low cost. Such applications include switching devices for active-matrix flat-panel displays (AMFPDs) based on either liquid crystal pixels (AMLCDs) [2] or organic light-emitting diodes (AMOLEDDs) [3, 4]. At present, hydrogenated amorphous silicon (a-Si:H) is the most commonly used active layer in TFT backplanes of AMLCDs. The higher performance of polycrystalline silicon TFTs is usually required for well-performing AMOLEDDs, but this field is still in the development stage; improvements in the efficiency of both the OLEDs and the TFTs could change this requirement. OTFTs could also be used in active-matrix backplanes for "electronic paper" displays [5] based on pixels comprising either electrophoretic ink-containing microcapsules [6] or "twisting balls" [7]. Other applications of OTFTs include low-end smart cards and electronic identification tags.

©Copyright 2001 by International Business Machines Corporation. Copying in printed form for private use is permitted without payment of royalty provided that (1) each reproduction is done without alteration and (2) the *Journal* reference and IBM copyright notice are included on the first page. The title and abstract, but no other portions, of this paper may be copied or distributed royalty free without further permission by computer-based and other information-service systems. Permission to *republish* any other portion of this paper must be obtained from the Editor.

0018-8646/01/$5.00 2001 IBM

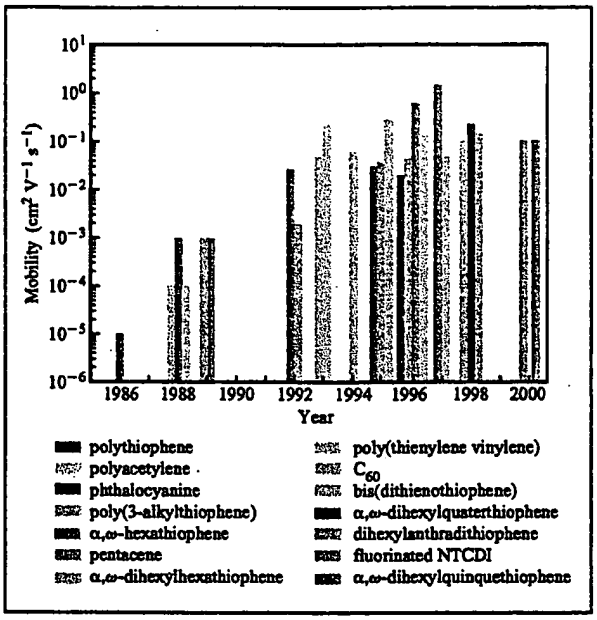

Semilogarithmic plot of the highest field-effect mobilities (μ) reported for OTFTs fabricated from the most promising polymeric and oligomeric semiconductors versus year from 1986 to 2000.

There are at least four ways in which a new, exploratory technology such as OTFTs can compete with or supplement a widely used, entrenched technology such as (a-Si:H) TFTs, for which many billions of dollars have already been invested:

1. *By far surpassing the performance of the entrenched technology and offering a substantial performance advantage.*
2. *By enabling an application that is not achievable using the entrenched technology, taking advantage of one or more unique properties or processing characteristics of OTFTs.* An example for Case 2 could be a flexible AMFPD fabricated on a plastic substrate. Because of the high processing temperature used in a-Si:H deposition (approximately 360°C), which is required for the fabrication of well-performing a-Si:H TFTs, it is not possible to fabricate an AMLCD based on such TFTs on a transparent plastic substrate. OTFTs, which can be processed at or close to room temperature and thus are compatible with transparent plastics, are an enabling technology which complements the entrenched technology instead of competing with it.
3. *By significantly reducing the cost of manufacturing OTFTs as compared to mainstream TFTs while delivering similar performance.*
4. *By leveraging a potential reduced cost advantage to create a new way of using an existing application, or to change the usage pattern or user habit for an existing application, even if performance is lower than that of the entrenched technology.* An example for Case 4 could be a large-area AMFPD which uses a backplane comprising OTFTs that have been fabricated using very low-cost processes compared to a-Si:H TFTs. Because of its significantly reduced cost, such a display could have a substantially reduced lifetime compared to a conventional AMFPD, since the user would be able to replace it several times over a period equal to the lifetime of a more expensive, conventional AMFPD.

Various forms of OTFTs can be applicable in all four modes of competition with the entrenched technology described above. Depending on the design of the OTFT and the specific materials and processes used to manufacture it, the cost and performance of the TFT can vary substantially. In this literature review an effort is made to describe this broad spectrum of materials, fabrication processes, designs, and applications of OTFTs, with an emphasis on papers published during the last three years. Older papers that, in the authors' opinion, played a very important role in shaping the OTFT field are also included, but the reader should look up a number of previously published review papers that cover that early period in more detail [8–14].

Progress in performance of OTFTs from 1986 to the present

In a previous paper [15] we presented a semilogarithmic plot of the highest yearly reported field-effect mobility value measured from thin-film transistors based on specific organic semiconductors, beginning in 1986. An update of that plot is shown in **Figure 1**, which is based on **Table 1**.

Table 1 lists the highest field-effect mobility (μ) values measured from OTFTs as reported in the literature, annually from 1986 through 2000 and separately for each of the most promising organic semiconductors. For a specific organic semiconductor that already has an entry in Table 1 and Figure 1 for a previous year, a new mobility value is entered only if it is higher than the value of the preceding entry. We can observe an impressive increase in mobility, which was achieved either by improving the processes used for the fabrication of the transistors or by synthesizing new organic materials. A typical path to performance increase could be described as a two-stage process: 1) A new organic semiconductor is synthesized or used for the first time as the active layer in an OTFT. 2) The film deposition parameters for the semiconducting organic layer are optimized to obtain the most advantageous structural and morphological characteristics for improved performance until no more improvement

Table 1 Highest field-effect mobility (μ) values measured from OTFTs as reported in the literature annually from 1986 through 2000.

Year	*Mobility* ($cm^2\ V^{-1}\ s^{-1}$)	*Material (deposition method)* (v) = vacuum deposition (s) = from solution	I_{on}/I_{off}*	*W/L*	*Reference*
1983	Minimal, not reported (NR)	Polyacetylene (s) (demonstration of field effect in an OTFT)	NR	200	[16]
1986	10^{-5}	Polythiophene (s)	10^3	NR	[17]
1988	10^{-4}	Polyacetylene (s)	10^5	750	[18]
	10^{-3}	Phthalocyanine (v)	NR	3	[19]
	10^{-4}	Poly(3-hexylthiophene) (s)	NR	NR	[20]
1989	10^{-3}	Poly(3-alkylthiophene) (s)	NR	NR	[21]
	10^{-3}	α–ω-hexathiophene (v)	NR	NR	[22]
1992	0.027	α–ω-hexathiophene (v)	NR	100	[23]
	2×10^{-3}	Pentacene (v)	NR	NR	ibid.
1993	0.05	α–ω-di-hexyl-hexathiophene (v)	NR	100–200	[24]
	0.22†	Polythienylenevinylene (s)	NR	1000	[25]
1994	0.06	α–ω-dihexyl-hexathiophene (v)	NR	50	[26]
1995	0.03	α–ω-hexathiophene (v)	$>10^6$	21	[27]
	0.038	Pentacene (v)	140	1000	[28]
	0.3	C_{60} (v)	NR	25	[29]
1996	0.02	Phthalocyanine (v)	2×10^5	NR	[30]
	0.045	Poly(3-hexylthiophene) (s)	340	20.8	[31]
	0.13	α–ω-dihexyl-hexathiophene (v)	$>10^4$	7.3	[15]
	0.62	Pentacene (v)	10^8	11	[32]
1997	1.5	Pentacene (v)	10^8	2.5	[33]
	0.05	Bis(dithienothiophene) (v)	10^8	500	[34]
1998	0.1	Poly(3-hexylthiophene) (s)	$>10^6$	20	[35]
	0.23	α–ω-dihexyl-quaterthiophene (v)	NR	1.5	[36]
	0.15	Dihexyl-anthradithiophene	NR	1.5	[37]
2000	0.1	n-decapentafluoroheptyl-methyl-naphthalene-1,4,5,8-tetracarboxylic diimide (v)	10^5	1.5	[38]
	0.1	α–ω-dihexyl-quinquethiophene (s)	NR	NR	[38]

*Values for I_{on}/I_{off} correspond to different gate voltage ranges and thus are not readily comparable to one another. The reader is encouraged to read the details of the experiments in the cited references.
†This result has not yet been reproduced.

seems possible. After that point, another incremental improvement in mobility usually is obtained from the synthesis and/or first OTFT application of a new organic semiconductor. This iterative procedure can be observed in Figure 1 by following the bars of the same color. Today, we have reached an important point in the plot of performance versus time. The most widely used organic semiconductors, such as pentacene, thiophene oligomers, and regioregular polythiophene, seem to have reached "maturity" as far as their performance is concerned. Their individual performance-versus-time curves have saturated (i.e., when a new, higher value is not reported in the years following a bar of a specific color, it means that there was no improvement in mobility during those years). In the past, each time such a performance saturation occurred (Figure 1), a new material was introduced whose performance broke the temporarily established upper limit in performance.

However, one can argue that today's maximum mobility at room temperature, which could be the field-effect mobility value of 2.7 $cm^2\ V^{-1}\ s^{-1}$ reported for holes in pentacene single crystals by Schön et al. [39], has approached a fundamental limit, at least as far as the classes of semiconducting organic materials known today are concerned. In the following section we discuss the potential existence of such a limit in conjunction with the various conduction mechanisms believed to be in operation in various organic semiconductors.

Conduction mechanisms and a potential fundamental limit to charge-carrier mobility in rganic semiconductors

The upper limits in microscopic mobilities of organic molecular crystals, determined at 300 K by time-of-flight experiments, are falling between 1 and 10 $cm^2 V^{-1} s^{-1}$ [40]. The weak intermolecular interaction forces in organic semiconductors, most usually van der Waals interactions with energies smaller than 10 kcal mol^{-1}, may be responsible for this limit, since the vibrational energy of the molecules reaches a magnitude close to that of the intermolecular bond energies at or above room temperature. In contrast, in inorganic semiconductors such as Si and Ge, the atoms are held together with very strong covalent bonds, which for the case of Si have energies as high as 76 kcal mol^{-1}. In these semiconductors, charge carriers move as highly delocalized plane waves in wide bands and have a very high mobility, as mentioned above ($\mu \gg 1$ $cm^2 V^{-1} s^{-1}$). The mobility is limited due to the scattering of carriers by lattice vibrations, and thus is reduced as temperature increases. Band transport is not applicable to disordered organic semiconductors, in which carrier transport takes place by hopping between localized states and carriers are scattered at every step. Hopping is assisted by phonons and mobility increases with temperature, although it is very low overall ($\mu \ll 1$ $cm^2 V^{-1} s^{-1}$).

The boundary between band transport and hopping is defined by materials having mobilities between 0.1 and 1 $cm^2 V^{-1} s^{-1}$ [13, 40, 41]. Highly ordered organic semiconductors, such as several members of the acene series including anthracene and pentacene, have room-temperature mobilities in this intermediate range, and in some cases temperature-independent mobility has been observed [40], even in polycrystalline thin films of pentacene [41]. That observation was used to argue that a simple temperature-activated hopping mechanism can be excluded as a transport mechanism in high-quality thin films of pentacene [41]. At low temperatures (below approximately 250 K), band transport becomes the mechanism that takes control of carrier transport in single crystals of pentacene and other acenes. Very high mobility values (from 400 $cm^2 V^{-1} s^{-1}$ [42] to more than 1000 $cm^2 V^{-1} s^{-1}$ [39]) have been reported. At these temperatures, the vibrational energy is much lower than the intermolecular bonding energy and phonon scattering is very low; thus, high mobility is exhibited. At or close to room temperature, phonon scattering becomes so high that the contribution of the band mechanism to transport becomes too small. At these same temperatures, hopping begins to contribute to carrier transport. Hopping of carriers from site to site becomes easier as the temperature rises. The combination of these two mechanisms explains the fact that the mobility decreases as temperature rises from a few degrees K to about 250 K, and after that the mobility begins to rise slowly [43]. This behavior is difficult or impossible to observe in polycrystalline films, in which traps attributed to structural defects dominate transport. Interestingly, a recent work [44] reports thermally activated transport for single crystals of pentacene, quaterthiophene, and hexathiophene isolated from polycrystalline films, which was attributed to Coulomb blockade-dominated transport. However, in the same work it was predicted that for materials with reduced tunnel resistance between the molecules, the Coulomb blockade model breaks down; as a result, mobilities greater than 0.5 $cm^2 V^{-1} s^{-1}$ and exhibiting temperature-independent behavior should be attainable. This is the case for the pentacene sample in Reference [41], which exhibited a mobility of 1.5 $cm^2 V^{-1} s^{-1}$ and had a temperature-independent mobility, in contrast to the sample having lower mobility ($\mu = 0.3$ $cm^2 V^{-1} s^{-1}$) and exhibiting thermally activated transport, a behavior that was attributed to thermally activated hopping conduction. There may be a reasonable explanation for the fact that the apparent mobility of the pentacene single crystal measured in Reference [44] is lower than the mobility of some polycrystalline films. It is possible that a trap-infested region is formed in the pentacene adjacent to the bottom electrodes, in the experiment of Reference [44]. We have shown that when pentacene is deposited on Au, as is the case in Reference [44], a microcrystalline, defect-infested region is formed in the channel, at and close to the edge of the gold electrode.[1] As a result of the existence of this region, there is a large concentration of traps close to the Au contact which dominates the carrier transport and drastically lowers the apparent mobility. These traps are also responsible for the gate-voltage dependence of the mobility of pentacene, as is also described below in more detail [45]. It is worth noting that the devices in Reference [41] had their source and drain electrodes deposited on top of the pentacene layer through a mask.

We can propose two possible ways of eliminating the potential fundamental limit at about 10 $cm^2 V^{-1} s^{-1}$ for the mobility of OTFTs, imposed by the weak intermolecular forces acting among nearest-neighbor (nn) molecules. One is to strengthen such interaction. This can be done by creating a stronger bond between nn molecules. However, this must take place without breaking the conjugation of the molecules. Stronger intermolecular bonds would result in stiffer crystalline structures, and thus it would take temperatures higher than room temperature to generate substantial scattering of highly delocalized carriers by lattice vibrations. Using such

[1] J. Kymissis, C. D. Dimitrakopoulos, and S. Purushothaman, *IEEE Transactions on Electron Devices*, in press.

a strategy, one could, in effect, produce at room temperature the high mobility that exists at very low temperatures in crystals of the acene series (e.g., pentacene). A second way would require more drastic change in the conduction path and mechanism. It would involve carrier transport along a single macromolecule that would bridge the gap between the source and drain electrodes of a TFT. Intermolecular conduction would give way to intramolecular conduction. It is well known that the mobility along the long axis of conjugated conducting and semiconducting polymers (e.g., polyacetylene) can reach values of 1000 $cm^2\ V^{-1}\ s^{-1}$ or more. This may require a drastic reduction in the size of the TFT channel from micron-size channels containing a large number of molecules to nano-size channels that are transcended by a single molecule. In the former case, conduction depends upon intermolecular transport, while in the latter, conduction takes place through the conjugated backbone of a single molecule and thus is intramolecular. The successful execution of at least one of the above strategies would prove that although limits can be imposed by the design and size of OTFT devices, they are not fundamental.

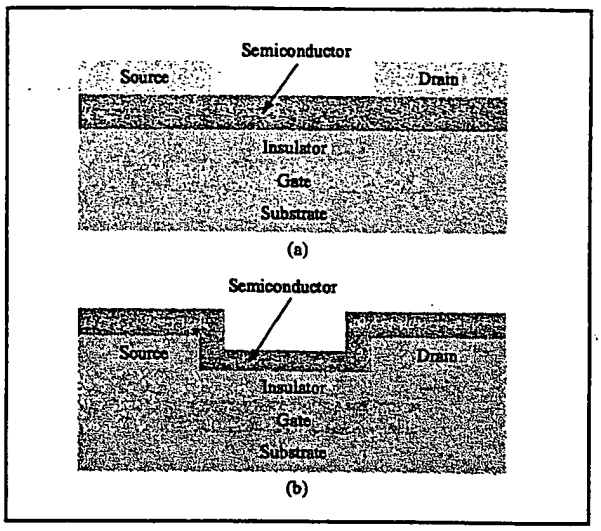

Figure 2

OTFT device configurations: (a) Top-contact device, with source and drain electrodes evaporated onto the organic semiconducting layer. (b) Bottom-contact device, with the organic semiconductor deposited onto prefabricated source and drain electrodes.

Modeling of the electrical characteristics of OTFTs

The majority of organic semiconductors exhibit p-type behavior; i.e., the majority carriers are holes (h^+). Their I–V characteristics can be adequately described by models developed for inorganic semiconductors [46], as shown earlier [11, 13, 15, 28, 47, 48]. An α–ω-dihexyl-hexathiophene (DH6T) TFT is used here to describe typical organic TFT device characteristics and the methods used to calculate the mobility and I_{on}/I_{off} ratio. **Figure 2** shows two common device configurations used in organic TFTs.

Figure 3(a) shows a typical plot of drain current I_D versus drain voltage V_D at various gate voltages V_G, which corresponds to a device using DH6T as the semiconductor, 3700 Å vapor-deposited parylene-C as the gate insulator, aluminum gate, and gold source and drain electrodes. When the gate electrode is biased negatively with respect to the grounded source electrode, DH6T insulated-gate field-effect transistors (IGFETs) operate in the accumulation mode and the accumulated charges are holes. At low V_D, I_D increases linearly with V_D (linear regime) and is approximately determined from the following equation:

$$I_D = \frac{WC_i}{L}\mu\left(V_G - V_T - \frac{V_D}{2}\right)V_D, \qquad (1)$$

where L is the channel length, W is the channel width, C_i is the capacitance per unit area of the insulating layer, V_T is the threshold voltage, and μ is the field-effect mobility. The latter can be calculated in the linear regime from the transconductance,

$$g_m = \left(\frac{\partial I_D}{\partial V_G}\right)_{V_D=\text{const}} = \frac{WC_i}{L}\mu V_D, \qquad (2)$$

by plotting I_D versus V_G at a constant low V_D and equating the value of the slope of this plot to g_m. **Figure 3(c)**, which corresponds to Figure 3(a), shows such a plot, and the calculated mobility value is 0.122 $cm^2\ V^{-1}\ s^{-1}$ at $V_D = -2$ V. The value of V_D is chosen so that it lies in the linear part of the I_D versus V_D curve. For this device, L was equal to 137 μm and W was equal to 1 mm. Other devices from the same substrate produced field-effect mobilities ranging from 0.095 to 0.131 $cm^2\ V^{-1}\ s^{-1}$.

When the gate electrode is biased positively, DH6T IGFETs operate in the depletion mode, and the channel region is depleted of carriers. The current modulation (the ratio of the current in the accumulation mode over the current in the depletion mode, also referred to as I_{on}/I_{off}) for the device of Figure 3 is slightly above 10^4 when V_G is scanned from −20 to +6 V [**Figure 3(b)**]. For V_D more negative than V_G, I_D tends to saturate (saturation regime) owing to the pinch-off of the accumulation layer, and is modeled by the equation

$$I_D = \frac{WC_i}{2L}\mu(V_G - V_T)^2. \qquad (3)$$

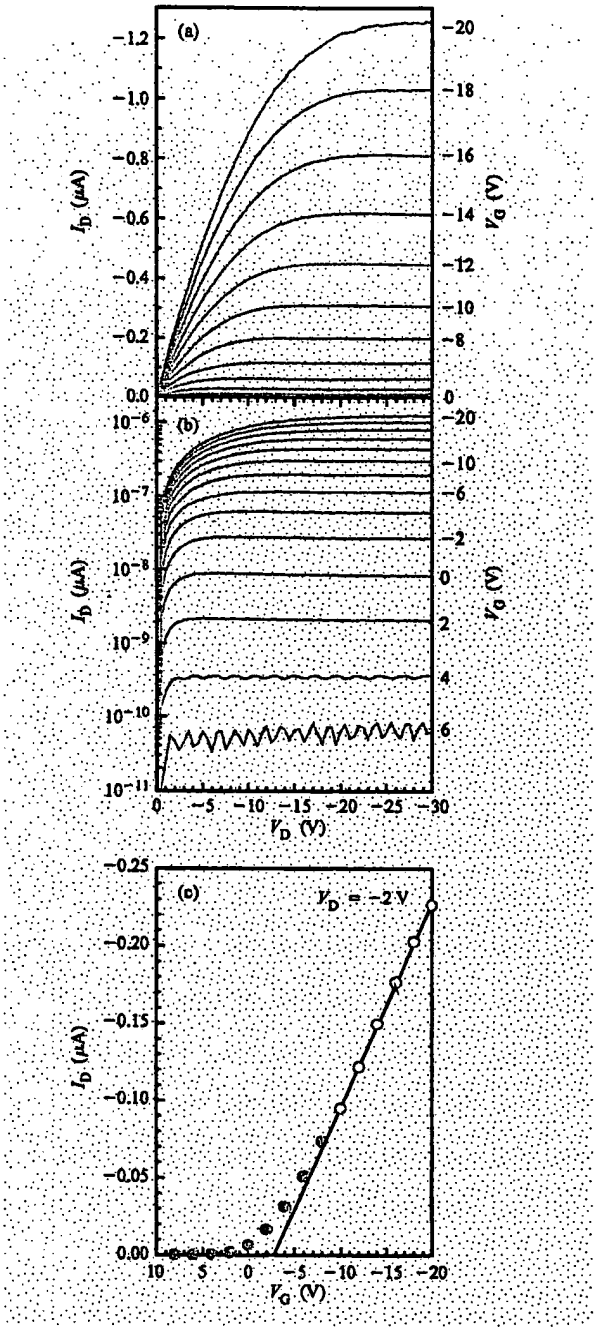

Device characteristics for a DH6T OTFT having an aluminum gate electrode, a 3700-Å vapor-deposited parylene-C gate insulating layer, and gold source and drain electrodes with L = 137 μm and W = 1 mm: (a) and (b) Drain current I_D versus drain voltage V_D for a range of gate-voltage values V_G plotted (a) linearly and (b) semilogarithmically; (c) I_D versus V_G at V_D = −2 V. Fitting this data to Equation (2) yielded a linear regime mobility of 0.122 cm^2 V^{-1} s^{-1}. Reprinted from [15] by permission of Elsevier Science.

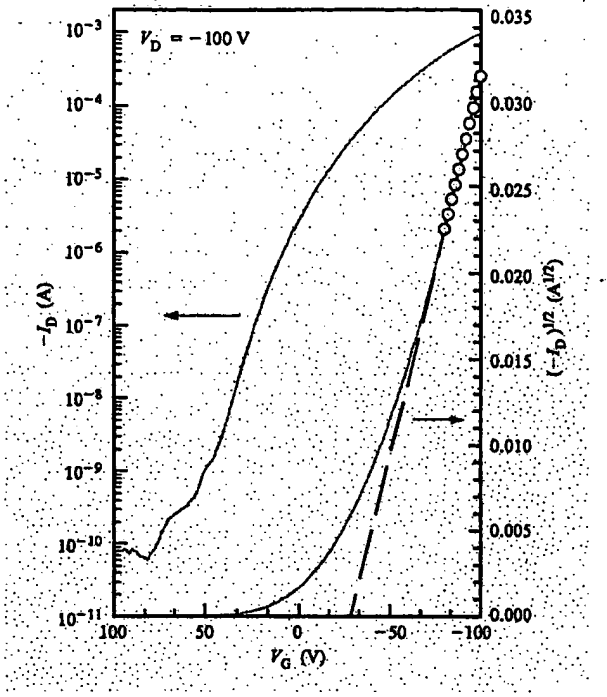

Drain current I_D versus gate voltage V_G and $|I_D|^{1/2}$ versus V_G for a pentacene OTFT having a heavily doped n-type Si gate electrode, 0.5 μm thermally grown SiO_2 gate insulator, and gold source and drain electrodes with L = 4.4 μm and W = 1.5 mm. Fitting $|I_D|^{1/2}$ versus V_G in the saturation regime (circles) using Equation (3) yielded a mobility of 0.16 cm^2 V^{-1} s^{-1}.

In the saturation regime, μ can be calculated from the slope of the plot of $|I_D|^{1/2}$ versus V_G. For the same device as in Figure 3, the mobility calculated in the saturation regime was 0.09 cm^2 V^{-1} s^{-1}.

Pentacene also exhibits typical p-type semiconductor characteristics. Figure 4 shows a graph that contains an I_D versus V_G plot and an $|I_D|^{1/2}$ versus V_G plot [45]. It corresponds to a device with channel length L = 4.4 μm and width W = 1500 μm, and utilizing pentacene as the semiconductor, 0.5-μm-thick thermally grown SiO_2 as the gate insulator, heavily doped Si (n-type) as the gate electrode, and gold source and drain electrodes. The field-effect mobility μ was 0.16 cm^2 V^{-1} s^{-1}, while the threshold voltage V_T was about −30 V. The I_{on}/I_{off} ratio was above 10^7 when V_G was scanned from −100 to +80 V. The measured mobility value is in agreement with reported hole mobilities from IGFETs based on pentacene films grown at room temperature [49, 50]. The mobility from devices with lower W/L ratios was considerably higher and reached 0.25 cm^2 V^{-1} s^{-1} for devices with W/L = 3.5

owing to fringe currents outside the channel. It is important that W/L be close to 10 or higher in order to minimize the effects of such currents; otherwise, the mobility is overestimated. An alternative way to achieve this would be to pattern the semiconductor so that its width does not exceed the width of the channel.

Differences can often be observed in mobility values calculated in the linear region and the saturation region. The linear region mobility can be affected by contact problems, and in such cases there are departures from the linearity of the I_D versus V_D curve which can lead to underestimation of mobility. In the saturation regime, when channel lengths are comparable to the gate insulator thickness or only a few times greater than that thickness, the I_D versus V_D curves do not saturate and exhibit an upward trend at high V_D. Calculating the mobility in the saturation region from such devices can lead to erroneously high values.

Vacuum-deposited organic semiconductor films

Pentacene TFTs have produced the highest performance among TFTs with an organic semiconducting channel (see Table 1). However, the operating voltage required to produce such performance (100 V) was too high, especially for portable applications that run on batteries. In a recent paper we studied the gate-voltage dependence of mobility in pentacene devices and used our understanding to demonstrate high-performance pentacene TFTs exhibiting high mobility and good current modulation at low operating voltages [45, 51]. For this purpose we employed a relatively high-dielectric-constant (ε) metal oxide film, barium zirconate titanate (BZT), as a gate insulator [45]. Our devices were fabricated using an all-room-temperature process. Additionally, we demonstrated full compatibility with transparent plastic substrates by fabricating devices on such substrates [45].

Figures 5(a) and 5(b) respectively show the dependence of field-effect mobility μ on the charge per unit area on the semiconductor side of the insulator Q_S, and the gate field E. The solid circles correspond to a pentacene-based device with a 0.12-μm-thick SiO_2 gate insulator thermally grown on the surface of a heavily doped n-type Si wafer that acted as the gate electrode. The open circles correspond to a similar device with a 0.5-μm-thick SiO_2 gate insulator. The mobility for the SiO_2-based devices is calculated in the saturation regime using a gate sweep, as explained in Figure 4, and is then plotted versus the maximum V_G used in each gate sweep. The maximum V_G is varied from -20 to -100 V. During all sweeps V_D is kept constant at -100 V in order to eliminate any effects that source and drain contact imperfections might have on our results. The mobility increases linearly with increasing Q_S and E and eventually saturates [Figures 5(a) and 5(b)].

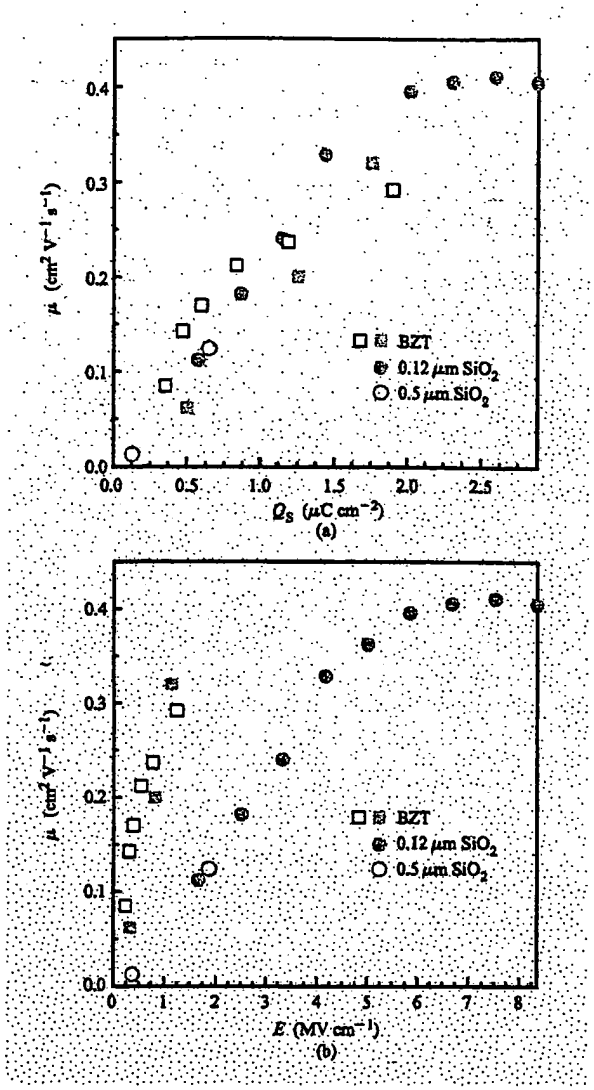

Figure 5

Dependence of field-effect mobility μ on (a) the charge per unit area on the semiconductor side of the insulator Q_S, and (b) the gate field E for pentacene OTFTs with different gate insulators.

Q_S is a function of the concentration of accumulated carriers in the channel region (N). Since the accumulation region has been shown in the past to be two-dimensional and confined very closely to the interface of the insulator with the organic semiconductor [52], all of this charge is expected to be localized within the first few semiconductor monolayers from this interface. An increase in V_G results in an increase in E and N. However, for the same V_G, N depends on both the dielectric constant and the thickness of the gate insulator, while E depends only on its

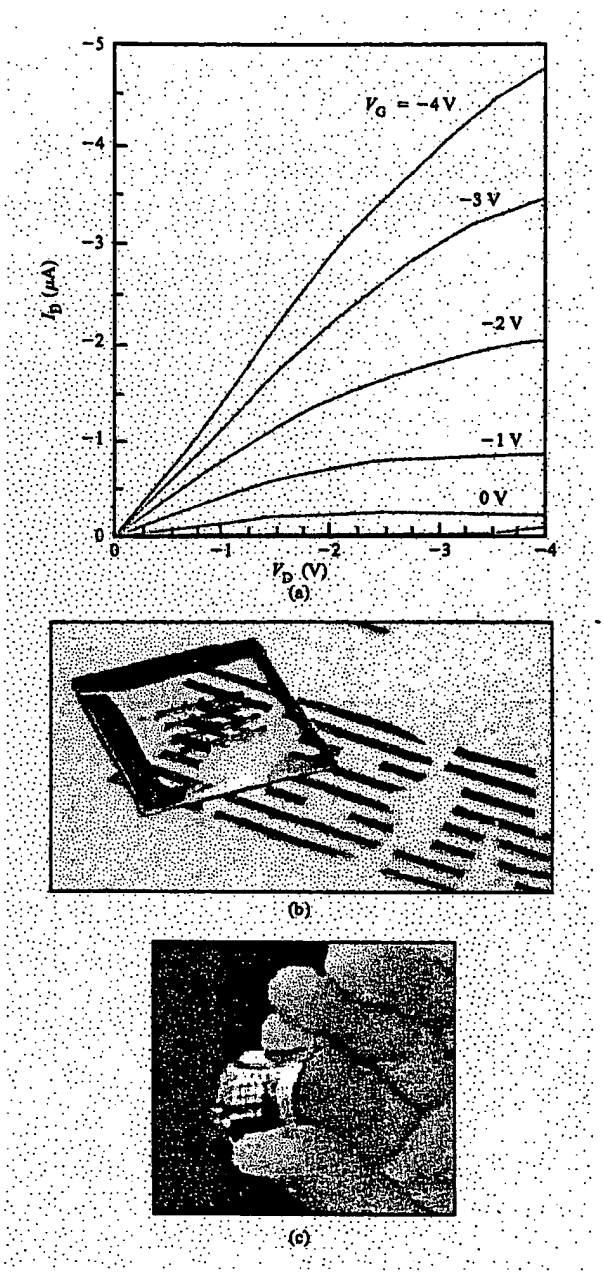

Figure 6

(a) Device characteristics for a pentacene TFT having a gold gate electrode, a 0.128-μm-thick sputtered BZT gate insulator, and gold source and drain electrodes with W = 1500 μm, L = 69.2 μm. Plot of drain current I_D versus drain voltage V_D for a range of gate-voltage values V_G. Data for this figure taken from [45]. (b) and (c) Photographs of the actual pentacene TFT devices on the polycarbonate substrate.

thickness. By replacing SiO_2 with an insulator having a similar thickness but a much higher dielectric constant, we facilitated charge accumulation. An accumulated carrier concentration similar to the SiO_2 case could be attained at much lower V_G, and hence E, with all of the other parameters being similar. If mobility depends on N rather than E, a high mobility should be achieved in the devices comprising the high-dielectric-constant gate insulator at much lower V_G, and hence E, than TFTs using a comparable thickness of SiO_2. Indeed, this is what we observe in Figure 5(b). The squares in Figure 5 correspond to devices comprising room-temperature-sputtered BZT as the gate insulator [45]. The solid squares are generated by gate sweeps, while the open squares are generated by drain sweeps. From Figure 5(b) it is obvious that the applied gate field used in BZT-based devices to obtain mobility values similar to those of the SiO_2-based devices was about five times lower than the fields used in the latter devices. This clearly proves that high field is not required to obtain high mobility. Thus, the gate-voltage dependence of mobility in these devices is due to the higher concentration of holes accumulated in the channel, which was achieved with the use of insulators having a higher dielectric constant. Figure 5(a), which plots μ versus charge per unit area, Q_S, shows exactly that. The values of Q_S and N required to reach a certain mobility value are practically the same for SiO_2- and BZT-based devices, although much different gate field values were required to obtain such a mobility in each case.

To prove the compatibility of our device-fabrication processes with transparent plastics, we have reported the successful fabrication of pentacene-based TFTs on thin, flexible polycarbonate substrates [45]. The BZT gate insulator used was 0.128 μm thick. The performance of these TFTs was similar to that of devices fabricated on quartz or SiO_2/Si substrates. **Figure 6(a)** shows the characteristics of such a device (W = 1500 μm, L = 69.2 μm) [45]. Mobility was 0.2 $cm^2\ V^{-1}\ s^{-1}$ as calculated in the saturation region [45]. Mobility values as high as 0.38 $cm^2\ V^{-1}\ s^{-1}$ were measured from devices with a W/L ratio of 4. These are the highest reported mobilities from devices fabricated on transparent plastic substrates and operating at a maximum voltage of only 4 V. **Figures 6(b)** and **6(c)** show the actual OTFT devices on the polycarbonate substrate.

In organic semiconductors, both the properties of the individual molecules and the structural order of the molecules in the film determine the macroscopic properties of the material. These properties can be controlled by using molecular engineering to synthesize molecules with optimal characteristics and by controlling the conditions under which these molecules assemble to form the solid. In the case of chain- or rod-like molecules, which have one molecular axis much longer than the other two, large π-conjugation length along the long axis and close molecular packing of the molecules along at least

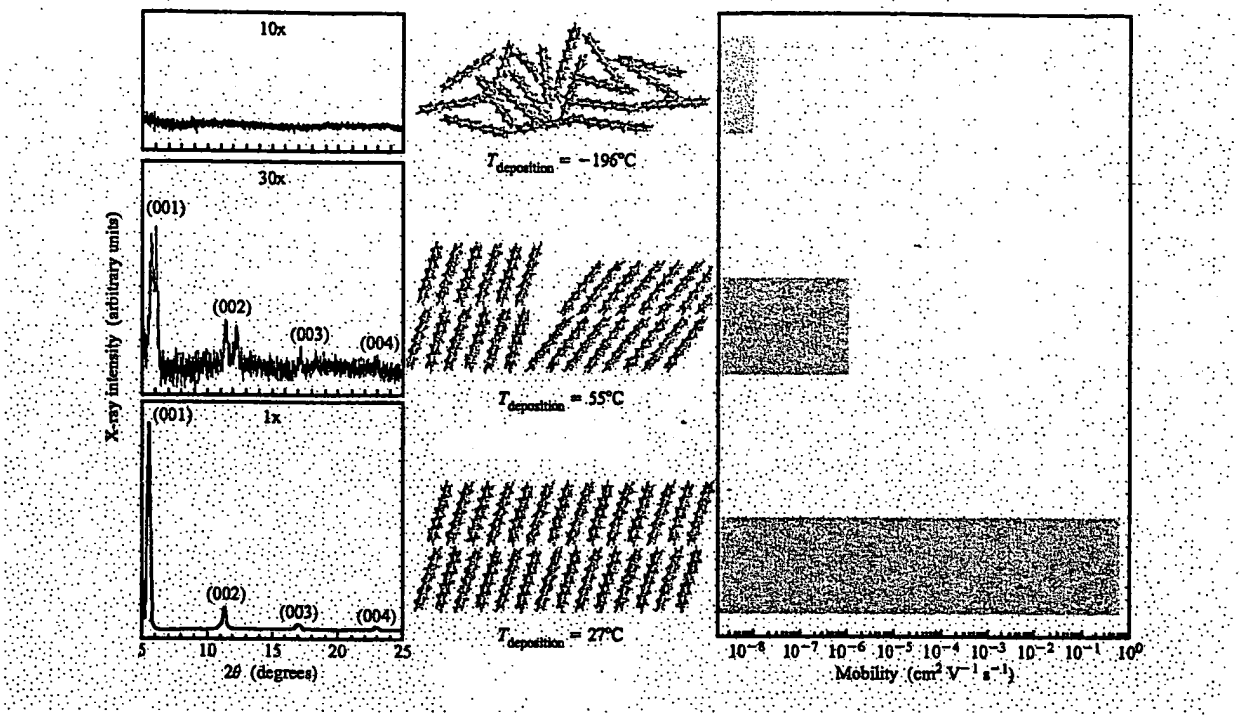

Comparison of X-ray diffraction patterns, schematic representations of structural order, and field-effect mobilities for three different phases of thin-film pentacene. An amorphous phase is achieved using a substrate temperature, $T_{deposition}$, of −196°C and a deposition rate DR of 0.5 Å s^{-1}. A single phase results at the temperature $T_{deposition}$ = 27°C and DR = 1 Å s^{-1}, while $T_{deposition}$ = 55°C and DR = 0.25 Å s^{-1} yields a double phase. Data partially taken from [28].

one of the short molecular axes are two important conditions for high carrier mobility. **Figure 7** contains proof of the above claims. By growing amorphous films of pentacene, which is achieved by keeping the substrate temperature low during deposition, we make a film that is practically insulating. When the substrate temperature is kept at room temperature during deposition, a very well-ordered film is deposited, and the mobility measured at room temperature is very high for an organic semiconductor (0.6 $cm^2 V^{-1} s^{-1}$). Since the structure of this thin film is different from the structure of single crystals of pentacene, we must distinguish between a "thin-film phase" and a "single-crystal phase" of pentacene. When a mixture of the thin-film phase and the single-crystal phase is grown [28], the mobility is very low, possibly because of the high defect concentration resulting from the coexistence of the two phases.

Pentacene transistor drain–source contacts can be made in one of two configurations [Figures 2(a) and 2(b)]: top contact and bottom contact. The performance of pentacene devices with the bottom-contact configuration is inferior to that of devices with the top-contact configuration. Consequently, most high-performance pentacene TFTs reported in the literature have the top-contact configuration, and shadow masking is generally used to pattern the source and drain contacts on top of the pentacene. This is a process that cannot be used in manufacturing. A process that allows the photolithographic patterning of the source and drain electrodes on the insulator before the deposition of pentacene, according to the schematic shown in Figure 2(b), had to be developed. Furthermore, the performance of devices fabricated with such a process should be similar to or better than that of top-contact devices [Figure 2(a)]. **Figure 8** shows a pentacene layer as it was grown on SiO_2 and a Au electrode. The edge between the SiO_2 and the Au in the middle photograph is marked by the end of the white (Au) area (due to variations in image contrast, the pentacene-covered Au appears different in the top two pictures). On SiO_2, far away from the Au edge, pentacene consists of fairly large grains (having sizes between 0.2 and 0.5 μm). On Au the grain size falls dramatically. Close to

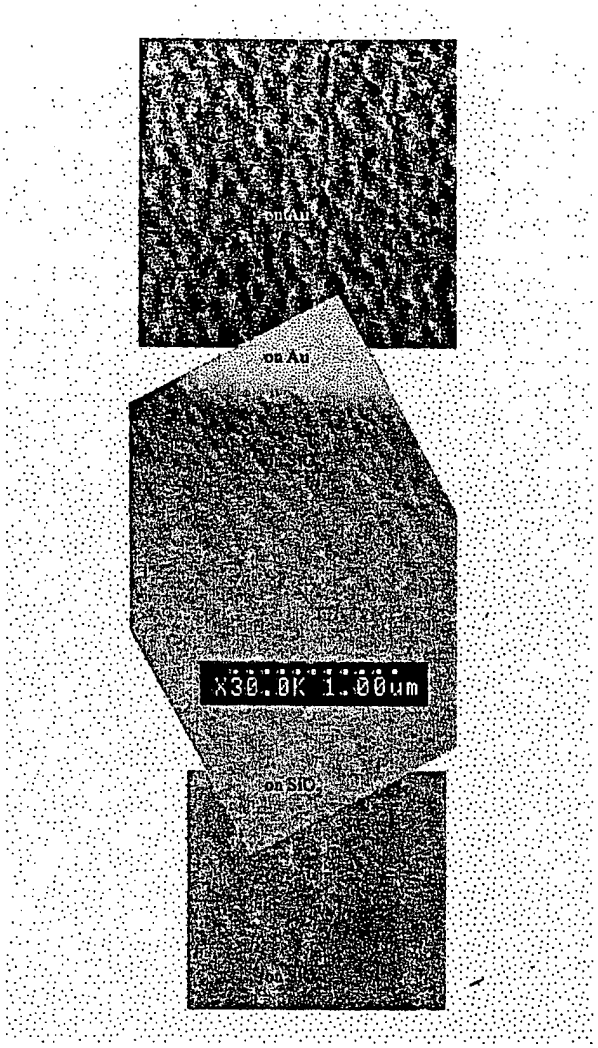

SEM image of a pentacene thin film grown on SiO_2 and an Au electrode. The grain size is much smaller on the Au than on the SiO_2 far from the Au edge. Near the Au edge, the grain size on the SiO_2 is similar to that on the Au and increases with increasing distance from the edge.

the Au edge but on the SiO_2 side, there is a transition region where the grain size increases with increasing distance from the edge.

In an organic TFT, the structure and contact behavior of the film formed on top of most of the electrode is not important for the performance of the device in the channel. It is the crystalline structure of pentacene at the electrode edge which causes the performance limitation of the bottom-contact TFT. Right at the edge of the Au electrode, there is an area with very small crystals and hence a large number of grain boundaries. Grain boundaries contain many morphological defects, which in turn are linked to the creation of charge-carrier traps with levels lying in the bandgap. These defects can be considered responsible for the reduced performance of bottom-contact pentacene TFTs. Their elimination should result in bottom-contact devices with performance similar to or better than that of top-contact devices. In a typical bottom-contact pentacene TFT, the mobility is equal to or less than 0.16 $cm^2\ V^{-1}\ s^{-1}$. We have used a self-assembled monolayer (SAM) of 1-hexadecane thiol to modify the surface energy of the Au electrode in an effort to improve the crystal size and ordering of the pentacene overgrowth.[1] The mobility calculated from such devices is 0.48 $cm^2\ V^{-1}\ s^{-1}$, which is three times larger than the mobility of the device with untreated Au electrodes. The pentacene layers for both devices were deposited in the same deposition run. **Figure 9** provides an explanation for the improvement in device performance. The SAM deposited on the Au resulted in a pentacene grain size on the Au similar to the large grains grown on the SiO_2. There is no transition region at the Au edge. The trap concentration must be drastically reduced.

Pentacene thin films are intolerant to exposure to the various chemicals used in typical lithographic processes; therefore, they cannot be patterned using such processes. Usually shadow masks are used during deposition to pattern the material. A technique was recently proposed which uses topographic discontinuities to isolate individual devices [53]. This technique requires that the semiconducting material and the photoresist remain in inactive areas, which can be a severe limitation for many applications. We have developed a subtractive technique in which pentacene is protected from the consequent lithographic steps by means of a chemically resistant layer.[2] A 1-μm-thick layer of parylene-N is first used to protect the sensitive pentacene layer from the solvents and other materials used. The two-layer structure thus formed is then etched using a typical lithographic process. Photoresist is spun on top of the structure and cured. The sample is then exposed to UV radiation through a lithographic mask and subsequently developed. The structure is then etched for 30 minutes in an oxygen plasma, resulting in well-defined patterns of protected pentacene on a clean substrate. Pentacene TFTs fabricated with this method had performance similar to that of shadow-mask-patterned pentacene devices fabricated in the same deposition run.

[1] J. Kymissis, C. D. Dimitrakopoulos, and S. Purushothaman, *IEEE Transactions on Electron Devices*, in press.
[2] J. Kymissis, C. D. Dimitrakopoulos, and S. Purushothaman, to be published.

Solution-processed organic semiconductor films

The technology that is believed to have the potential to produce the highest impact on manufacturing costs is the use of soluble organic semiconductors, both polymers and oligomers, combined with large-area stamping or printing techniques that could eliminate lithography. Below, we summarize some of the important developments in this field.

One of the first solution-processable organic semiconductors used for field-effect transistors was poly(3-hexylthiophene) [20]. Poly(3-hexylthiophene) films spun from chloroform onto interdigitated gold source and drain electrodes displayed mobilities in the range of 10^{-5} to 10^{-4} $cm^2\ V^{-1}\ s^{-1}$. These mobilities were comparable to the mobilities obtained from electrochemically prepared polythiophene field-effect transistors [54], indicating that the incorporation of insulating alkyl side chains was not detrimental to the electronic properties of polythiophene. A comparison study of poly(3-alkylthiophene)s with side chains ranging in length from butyl to decyl showed that field-effect mobility decreases with increasing chain length [55]. For films spun from chloroform, mobilities ranged from 1 to 2×10^{-4} $cm^2\ V^{-1}\ s^{-1}$ for poly(3-butylthiophene) and poly(3-hexylthiophene) down to 6×10^{-7} $cm^2\ V^{-1}\ s^{-1}$ for poly(3-decylthiophene).

A dramatic increase in mobility was observed when regioregular poly(3-hexylthiophene), synthesized by the Reike method [56] and having greater than 98.5% head-to-tail (HT) linkages, was used to fabricate a field-effect transistor [31]. Poly(3-hexylthiophene) can have the 3-alkyl substituents incorporated into the polymer in two types of arrangements: head to tail and head to head (HH). If poly(3-hexylthiophene) consists of both HH and HT 3-alkylthiophene moieties, it is regiorandom. Regioregular poly(3-hexylthiophene) has only one type of arrangement, either HH or HT. Mobilities as high as 0.045 $cm^2\ V^{-1}\ s^{-1}$ were achieved when regioregular poly(3-hexylthiophene) was solution-cast (i.e., drop-cast) from a chloroform solution. When cast from solution, highly regioregular poly(3-hexylthiophene) self-orients into a well-ordered lamellar structure with an edge-on orientation of the thiophene rings relative to the substrate. This is in contrast to solution-cast films of regiorandom poly(3-alkylthiophene)s, which are totally amorphous [56]. Spin-coated films of regioregular poly(3-hexylthiophene) are also well-ordered, but the lamellae adopt different orientations depending on the degree of regioregularity [57]. Highly regioregular poly(3-hexylthiophene) (greater than 91% head-to-tail linkages) forms lamellae with an edge-on orientation (π–π stacking direction in the plane of the substrate) when spun from chloroform. Mobilities of 0.05 to 0.1 $cm^2\ V^{-1}\ s^{-1}$ were obtained for 96% regioregular poly(3-hexylthiophene). In contrast, spun films of poly(3-hexylthiophene) with low regioregularity (81% head-to-tail linkages) consisted of lamellae having a face-on orientation (π–π stacking direction perpendicular to the substrate) and gave mobilities of 2×10^{-4} $cm^2\ V^{-1}\ s^{-1}$. Solution-cast films of 81% regioregular poly(3-hexylthiophene) adopted an edge-on lamellar structure, resulting in an order-of-magnitude increase in mobility compared to spin-coated films. This study indicates that, in addition to the degree of order of the polymer film, the orientation of the π–π stacking direction relative to the substrate has a large influence on the field-effect mobility.

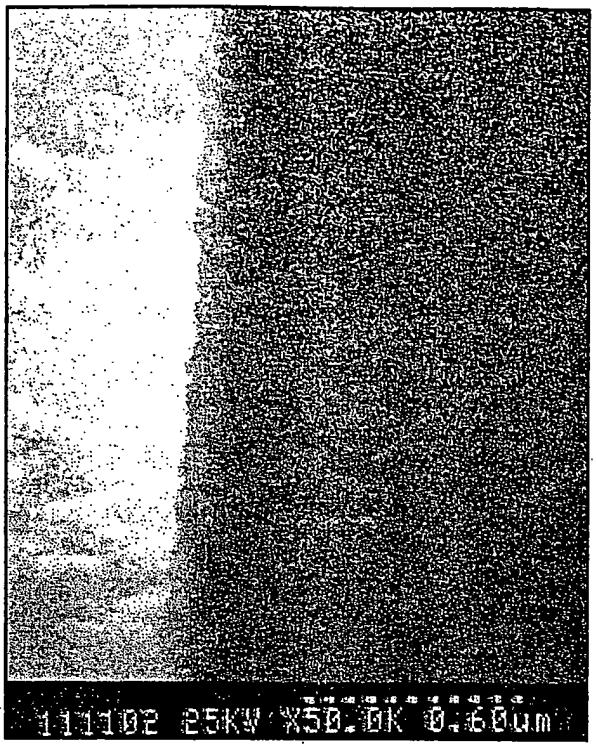

Figure 5

SEM image of a pentacene thin film grown on SiO_2 and a surface-modified Au electrode. The self-assembled monolayer of 1-hexadecane thiol resulted in a similar grain size on both the SiO_2 and the Au and eliminated the size transition region at the Au edge. (J. Kymissis, C. D. Dimitrakopoulos, and S. Purushothaman, *IEEE Transactions on Electron Devices*, in press.)

A variety of solvents have been investigated for the deposition of thin films of regioregular poly(3-alkylthiophene)s, including chloroform, 1,1,2,2-tetrachloroethane, tetrachloroethylene, chlorobenzene, toluene, *p*-xylene, and THF. The various solvents produce films with different degrees of order, uniformity, and continuity. The mobility of regioregular poly(3-hexylthiophene) was found to vary by two orders

of magnitude depending on the solvent used, with chloroform giving the highest mobility [56]. Modification of the substrate surface prior to deposition of regioregular poly(3-alkylthiophene) has also been found to influence film morphology. For example, treatment of SiO_2 with hexamethyldisilazane (HMDS) or an alkyltrichlorosilane replaces the hydroxyl groups at the SiO_2 surface with methyl or alkyl groups. The apolar nature of these groups apparently attracts the hexyl side chains of poly(3-hexylthiophene), favoring lamellae with an edge-on orientation. Mobilities of 0.05 to 0.1 $cm^2\ V^{-1}\ s^{-1}$ from highly regioregular poly(3-hexylthiophene) have been attributed to this surface modification process [35, 57, 58]. In addition, it has been shown that deposition onto a flat substrate (top-contact device) is favorable compared to deposition onto prefabricated source and drain electrodes (bottom-contact device), yielding mobilities that are typically larger by a factor of 2 [35, 58].

Several processing techniques have been found to enhance the on–off switching characteristics of poly(3-alkylthiophene) field-effect devices without affecting their mobility. Treatment of a poly(3-hexylthiophene) solution-cast film with ammonia by bubbling N_2 through an aqueous ammonium hydroxide solution for ten hours increased the on–off ratio by more than an order of magnitude. Short thermal treatments in a N_2 atmosphere were also found to reduce the off current slightly, but higher temperatures (~150°C) caused nearly an order of magnitude decrease in mobility [31]. Evaporation of a thin layer of SiO_x onto the poly(3-alkylthiophene) film has been shown to increase the on–off ratio by as much as four orders of magnitude. Immersing the film in hydrazine has a similar effect. Both substoichiometric SiO_2 and hydrazine are reducing agents which act to dedope the poly(3-alkylthiophene) film [35, 58]. Exposure of poly(3-alkylthiophene) films to air causes an increase in conductivity and a subsequent degradation of the transistor on–off characteristics. It is possible to achieve high on–off ratios by preparing and testing devices in a dry N_2 atmosphere [35, 58].

Although most studies have focused on poly(3-hexylthiophene), other regioregular poly(3-alkylthiophene)s have also been used to fabricate field-effect transistors. Poly(3-octylthiophene) was found to have a field-effect mobility similar to that of poly(3-hexylthiophene), 0.01 to 0.03 $cm^2\ V^{-1}\ s^{-1}$ for devices with an indium–tin oxide (ITO) [on poly(ethylene terephthalate)] gate, polyimide insulating layer, and top-contact conductive ink source and drain electrodes. For this same device configuration, the mobility of regioregular poly(3-dodecylthiophene) was only $10^{-6}\ cm^2\ V^{-1}\ s^{-1}$ [59]. This trend of decreasing mobility with increasing side chain length is the same as was observed in a series of regiorandom poly(3-alkylthiophene)s [55].

In addition to the variation of alkyl side-chain length, modification of the chemical nature of the side chains in regioregular substituted polythiophenes has also been investigated [60]. Carboxylic acid side chains were incorporated in an attempt to use hydrogen bonding to aid self-orientation at polar substrate surfaces (e.g., SiO_2). However, solution-cast films of this polymer were nonuniform and essentially amorphous, and mobilities were in the range of 10^{-5} to $10^{-4}\ cm^2\ V^{-1}\ s^{-1}$. A similar lack of crystallinity and low mobilities were observed in cast films of regioregular polythiophenes with bulky oxazoline side chains. The introduction of an optically active methyl branch off a butyl side chain produced crystalline films and field-effect mobilities of $10^{-3}\ cm^2\ V^{-1}\ s^{-1}$. The increased π–π stacking distance caused by the methyl branch is thought to be responsible for the reduction of the mobility by one to two orders of magnitude compared to regioregular polythiophenes with unbranched alkyl side chains.

While spin coating, solution casting, and printing are perhaps the most commercially feasible processing techniques for soluble polymeric semiconductors, the Langmuir–Blodgett (LB) technique has also been explored for the preparation of poly(3-alkylthiophene) field-effect transistors [61–63]. Initial LB studies used mixtures of regiorandom poly(3-hexylthiophene) and arachidic acid. Substantial molar percentages of the long-chain fatty acid were necessary for the formation of stable Langmuir films at the air–water interface and subsequent vertical transfer onto a transistor substrate [61, 62]. Mobilities ranged from 10^{-7} to $10^{-4}\ cm^2\ V^{-1}\ s^{-1}$ for multilayer LB films, and were even lower for monolayer films. These low mobilities are not surprising considering the regiorandom nature of the polymer and the insulating nature of the fatty acid. A subsequent study showed that it is possible to form a stable Langmuir monolayer of regioregular poly(3-hexylthiophene) without the addition of a long-chain fatty acid [63]. Transistors were fabricated by horizontal (Langmuir–Schaeffer) deposition onto hydrophobic substrates. The transferred films displayed a layered structure with an edge-on orientation of the thiophene rings, and were more or less ordered depending on the spreading solvent used. Mobilities ranged from 3×10^{-3} to $2 \times 10^{-2}\ cm^2\ V^{-1}\ s^{-1}$ for multilayer films (2–5 layers) and were lower for monolayers. Although optical characterization of the films indicated a tendency of the polymer backbones to align parallel to the trough barriers, this anisotropy was not apparent in the electrical measurements. The difficulty of vertical transfer of LB monolayers of regioregular poly(3-alkylthiophene)s has been addressed by chemically modifying the side chains in order to make the polymer amphiphilic [64]. The introduction of perfectly alternating dodecyl (hydrophobic)

and trioxynonyl (hydrophilic) groups allows vertical deposition of a monolayer onto a hydrophilic substrate with a transfer ratio of 1.0 ± 0.1. It is also possible to form a patterned polymer layer by deposition onto a substrate with patterned hydrophilic and hydrophobic areas. Such amphiphilic, regioregular polythiophenes are promising materials for LB field-effect transistors, especially if transfer ratios remain near unity for the deposition of a few multilayers.

Field-effect mobilities of vacuum-evaporated oligothiophenes, especially end-substituted oligothiophenes, are among the highest reported for organic semiconductors, with the exception of pentacene. Unsubstituted quinquethiophene and end-substituted quater-, quinque-, and hexathiophene display enough solubility in organic solvents to allow fabrication of field-effect devices by solution-processing techniques. Initial studies of solution-processed oligothiophene transistors gave mobilities of $\sim 5 \times 10^{-5}$ cm^2 V^{-1} s^{-1} for quinquethiophene and α,α'-diethylquaterthiophene (DE4T) [65]. Evaporated films of DE4T yielded only slightly higher mobilities, of the order of 9×10^{-5} cm^2 V^{-1} s^{-1}. According to X-ray diffraction studies, both evaporated films and films solution-cast from chloroform were highly crystalline, with the DE4T molecules arranged in a layered structure [65].

More recently, mobilities in the range of 10^{-2} to 10^{-1} cm^2 V^{-1} s^{-1} have been achieved using solution-processed substituted oligothiophenes [38, 66, 67]. Not surprisingly, the mobility is found to depend strongly on film morphology, which can be controlled by the processing conditions. In one study, α,α'-dihexylhexathiophene (DH6T) and α,α'-dihexylquaterthiophene (DH4T) were dissolved in hot chlorobenzene or 1,2,4-trichlorobenzene, then solution-cast onto bottom-contact substrates. The solvent was evaporated in a vacuum oven at temperatures between room temperature and 100°C. The resulting films were nonuniform in both thickness and morphology and yielded a range of mobilities. For DH6T films prepared in this way, the mobilities ranged from 4×10^{-3} to 5×10^{-2} cm^2 V^{-1} s^{-1}, with the highest mobilities corresponding to trichlorobenzene and 70°C solvent evaporation. The mobilities of DH4T films were less consistent, ranging from 1×10^{-3} to 7×10^{-2} cm^2 V^{-1} s^{-1}, but generally slightly lower than those of DH6T films prepared under the same conditions [66]. In another study, additional solvents were investigated, including 3-methylthiophene, anisole, and toluene. After DH6T was dissolved in hot solvent, the solution was cast onto a heated (50–60°C) substrate, and the solvent was evaporated under partial vacuum. Chlorobenzene, 1,2,4-trichlorobenzene, and 3-methylthiophene all yielded smooth films and mobilities occasionally as high as 0.1 cm^2 V^{-1} s^{-1} and routinely 0.03 cm^2 V^{-1} s^{-1} when the DH6T concentration was less than 0.1%. For higher concentrations, the films were thicker but rough and gave low mobilities. The less polarizable solvents anisole and toluene did not produce smooth films because the DH6T precipitated from the solution prior to any nucleation at the substrate surface. A mobility of 0.03 cm^2 V^{-1} s^{-1} was also obtained from a film of α,α'-dihexylquinquethiophene (DH5T) cast from chlorobenzene onto a 50°C substrate [67]. A subsequent study reported a mobility of 0.1 cm^2 V^{-1} s^{-1} from a DH5T film solution-cast from toluene [38].

High mobilities (1.2×10^{-2} cm^2 V^{-1} s^{-1}) have also been reported for films of DH4T spun from chloroform [68]. A polycrystalline film of DH4T resulted when the SiO_2 substrate was first treated with *n*-octyltrichlorosilane to make the surface hydrophobic and then held at 110°C while the film was being spun. Differential scanning calorimetry (DSC) measurements indicate that DH4T is in a liquid-crystalline phase at this temperature, and this apparently facilitates long-range molecular organization. The mobilities of films prepared by spin-coating in this manner are only slightly lower than the mobilities of vacuum-evaporated films of DH4T, which are of the order of 3×10^{-2} cm^2 V^{-1} s^{-1}. Chemical modification of end-substituted thiophene oligomers to have alkoxypropyl instead of alkyl end groups has been investigated as a means of increasing oligomer solubility. In particular, field-effect transistors were fabricated from quaterthiophene and hexathiophene end-substituted with 3-butoxypropyl groups, C4OC3α4T and C4OC3α6T [38]. The solubility of these oligomers was increased by as much as a factor of 2 compared to the corresponding alkyl-substituted oligomers. C4OC3α4T and C4OC3α6T were solution-cast from chlorobenzene or 1,2,4-trichlorobenzene, and the solvent was evaporated in a vacuum oven. Although the incorporation of an oxygen atom into the end group did not seem to affect the packing and spacing of molecules in cast films, the mobilities for C4OC3α6T (1×10^{-3} to 1×10^{-2} cm^2 V^{-1} s^{-1}) were slightly lower than those of DH6T, and the mobilities for C4OC3α4T (5×10^{-5} to 1×10^{-3} cm^2 V^{-1} s^{-1}) were significantly lower than those of DH4T.

Other soluble organic oligomers have also been investigated as semiconducting materials for field-effect transistors. Anthradithiophene, a fused heterocycle compound similar to pentacene, is soluble in its dihexyl end-substituted form. Dihexylanthradithiophene (DHADT) transistors were fabricated by solution-casting from hot chlorobenzene, then evaporating the solvent in a vacuum oven at various temperatures. The electrical characteristics of the films were strongly dependent on the solvent evaporation temperature, with no field effect observed for room temperature, 50°C, 150°C, or 180°C. For films dried at 70°C, mobilities ranged from 6×10^{-4} to 3×10^{-3} cm^2 V^{-1} s^{-1}. The highest mobilities, 0.01 to 0.02 cm^2 V^{-1} s^{-1},

were obtained for a drying temperature of 100°C [37, 67]. In comparison, vacuum-evaporated films of DHADT gave mobilities as high as 0.15 $cm^2 V^{-1} s^{-1}$ [37]. Transistors utilizing another thiophene-containing oligomer, *trans-trans*-2,5-bis-[2-{5-(2,2'-bithienyl)}ethenyl]thiophene (BTET), were fabricated by spin-coating from hot NMP. The mobility of such a device was 1.4×10^{-3} $cm^2 V^{-1} s^{-1}$ compared to 0.012 $cm^2 V^{-1} s^{-1}$ for a vacuum-evaporated device [69].

Most organic semiconductors, including the thiophene oligomers discussed above, are p-type semiconductors. However, a naphthalenetetracarboxylic diimide derivative with fluorinated R groups has been reported as a solution-processable n-type organic semiconductor [38]. This compound is soluble in hot α,α,α-trifluorotoluene, and solution-casting results in morphologically nonuniform films, with some regions of the films giving mobilities greater than 0.01 $cm^2 V^{-1} s^{-1}$. Vacuum-deposited films yielded higher mobilities.

Although a great deal of success has been achieved with soluble oligomers, the solubilities of these oligomers are low, requiring the solvents to be heated, and casting and spinning yield films that are nonuniform in thickness, morphology, and electrical properties. Another approach to solution-processable oligomeric materials is to begin with a precursor molecule that is soluble but not semiconducting, and then convert it to its semiconducting, insoluble form. This approach has been realized for pentacene, with initial mobilities of 0.01 to 0.03 $cm^2 V^{-1} s^{-1}$ reported [11, 70, 71]. The pentacene precursor is soluble in dichloromethane and forms continuous, amorphous films when spun onto transistor substrates. The conversion to pentacene is accomplished by heating the films to a temperature of 140–220°C in vacuum for several minutes to two hours. Tetrachlorobenzene is eliminated in the conversion process, and electron microscopy reveals microcrystallites in the converted films. In a subsequent study, a mobility of 0.2 $cm^2 V^{-1} s^{-1}$ was achieved by treatment of the SiO_2 substrate with HMDS prior to spin-coating the precursor, and by optimizing the conversion conditions. These optimized conditions involved spinning the precursor from a 1.5 wt% solution in dichloromethane and converting the film for five seconds at 200°C, followed by rapid quenching [72].

This precursor approach can also be applied to polymers. In fact, one of the first reported organic transistors used precursor-route polyacetylene as the semiconducting layer. The polyacetylene precursor was spun from cold 2-butanone, and conversion was achieved by heating to 80–100°C in vacuum for 12 hours. The mobilities of such transistors were low, however, in the range of 10^{-4} to 10^{-5} $cm^2 V^{-1} s^{-1}$ [18, 73]. Another polymeric semiconductor that has been processed from a soluble precursor polymer is polythienylenevinylene (PTV). In an initial study, a PTV film was spun from dimethylformamide and then coated with a layer of precursor poly(*p*-phenylene vinylene) (PPV). Both the PTV and PPV were converted at 100–300°C in a N_2 atmosphere, with the PPV precursor supplying protons to catalyze the PTV conversion. A mobility of 6×10^{-4} $cm^2 V^{-1} s^{-1}$ was reported for a device prepared in this way [54]. Subsequent studies have spun the PTV precursor from chloroform and dichloromethane, and have converted the PTV at 140–160°C in a N_2 atmosphere with a flow of HCl gas to catalyze the reaction [11, 71, 74]. Although the mobilities remain fairly low, in the range of 10^{-4} to 10^{-3} $cm^2 V^{-1} s^{-1}$, one advantage of this processing approach is that organic solvents can be used in subsequent device-processing steps without disturbing the converted PTV [74].

Conclusions

There has been tremendous progress in OTFT performance during the last decade. At present, we have reached the point at which an initial product application can be seriously considered. Organic semiconductors such as pentacene, deposited by vacuum sublimation, remain the best performers because of their very well ordered structures, resulting from the use of this highly controllable deposition method. However, substantial improvements have taken place in solution-processed organic semiconductors, and their mobilities are currently only one order of magnitude lower than those of vapor-deposited pentacene TFTs. There is a potentially important cost advantage associated with the solution processing of organic TFTs, because it eliminates the need for expensive vacuum chambers and lengthy pump-down cycles. However, for this advantage to be realized, all or at least most of the layers comprising the TFT device should be deposited using methods that do not involve vacuum deposition. These layers include the source, drain, and gate electrodes that currently are fabricated from high-work-function metals, the gate dielectric, and the (potentially necessary for some materials) passivation/encapsulation layer. Reel-to-reel processing, which is the most promising fabrication process for reducing costs, can be applied to both vacuum- and solution-deposited organic semiconductors; thus, it does not constitute an exclusive advantage for either of the two classes of materials.

All in all, organic TFTs are close to passage from the research laboratory to product development and then to manufacturing of new products based on organic semiconductors.

References

1. Y. Taur and T. H. Ning, *Fundamentals of Modern VLSI Devices*, Cambridge University Press, New York, 1998, p. 11.
2. K. Schleupen, P. Alt, P. Andry, S. Asaad, E. Colgan, P. Fryer, E. Galligan, W. Graham, P. Greier, R. Horton, H. Ifill, R. John, R. Kaufman, H. Kinoshita, H. Kitahara, M. Kodate, A. Lanzetta, K. Latzko, S. Libertini, F. Libsch, A. Lien, M. Mastro, S. Millman, R. Nunes, R. Nywening, R. Polastre, J. Ritsko, M. Rothwell, S. Takasugi, K. Warren, J. Wilson, R. Wisnieff, S. Wright, and C. Yue, "High Information Content Color 16.3" Desktop AMLCD with 15.7 Million a-Si:H TFTs," *Proceedings of the 18th International Display Research Conference, Asia Display '98*, 1998, pp. 187–190.
3. W. Riess, H. Riel, T. Beierlein, W. Brütting, P. Müller, and P. F. Seidler, "Influence of Trapped and Interfacial Charges in Organic Multilayer Light-Emitting Devices," *IBM J. Res. & Dev.* 45, 77 (2001, this issue).
4. R. Friend, J. Burroughes, and T. Shimoda, "Polymer Diodes," *Phys. World* (UK) 12, 35 (1999).
5. R. Wisnieff, "Printing Screens," *Nature* 394, 225 (1998).
6. B. Comiskey, J. D. Albert, H. Yoshizawa, and J. Jacobson, "An Electrophoretic Ink for All-Printed Reflective Electronic Displays," *Nature* 394, 253 (1998).
7. N. K. Sheridon, U.S. Patent 4,126,854, 1978.
8. N. Greenham and R. H. Friend, in *Solid State Physics: Advances in Research and Applications*, Vol. 49, H. Ehrenreich and F. Spaepen, Eds., Academic Press, San Diego, 1995, pp. 1–149.
9. A. J. Lovinger and L. J. Rothberg, "Electrically Active Organic and Polymeric Materials for Thin-Film-Transistor-Applications," *J. Mater. Res.* 11, 1581 (1996).
10. H. E. Katz, "Organic Molecular Solids as Thin Film Transistor Semiconductors," *J. Mater. Chem.* 7, 369 (1997).
11. A. R. Brown, C. P. Jarrett, D. M. de Leeuw, and M. Matters, "Field-Effect Transistors Made From Solution-Processed Organic Semiconductors," *Synth. Met.* 88, 37 (1997).
12. F. Garnier, "Thin Film Transistors Based On Organic Conjugated Semiconductors," *Chem. Phys.* 227, 253 (1998).
13. G. Horowitz, "Organic Field-Effect Transistors," *Adv. Mater.* 10, 365 (1998).
14. H. E. Katz and Z. Bao, "The Physical Chemistry of Organic Field-Effect Transistors," *J. Phys. Chem. B* 104, 671 (2000).
15. C. D. Dimitrakopoulos, B. K. Furman, T. Graham, S. Hegde, and S. Purushothaman, "Field-Effect Transistors Comprising Molecular Beam Deposited α–ω-Di-hexyl-hexathienylene and Polymeric Insulators," *Synth. Met.* 92, 47 (1998).
16. F. Ebisawa, T. Kurokawa, and S. Nara, "Electrical Properties of Polyacetylene/Polysiloxane Interface," *J. Appl. Phys.* 54, 3255 (1983).
17. A. Tsumura, H. Koezuka, and T. Ando, "Macromolecular Electronic Device: Field-Effect Transistor with a Polythiophene Thin Film," *Appl. Phys. Lett.* 49, 1210 (1986).
18. J. H. Burroughes, C. A. Jones, and R. H. Friend, "New Semiconductor Device Physics in Polymer Diodes and Transistors," *Nature* 335, 137 (1988).
19. C. Clarisse, M. T. Riou, M. Gauneau, and M. Le Contellec, "Field-Effect Transistor with Diphthalocyanine Thin Film," *Electron. Lett.* 24, 674 (1988).
20. A. Assadi, C. Svensson, M. Willander, and O. Inganäs, "Field-Effect Mobility of Poly(3-hexylthiophene)," *Appl. Phys. Lett.* 53, 195 (1988).
21. J. Paloheimo, E. Punkka, H. Stubb, and P. Kuivalainen, in *Lower Dimensional Systems and Molecular Devices, Proceedings of NATO ASI*, Spetses, Greece, R. M. Mertzger, Ed., Plenum Press, New York, 1989.
22. G. Horowitz, D. Fichou, X. Peng, Z. Xu, and F. Garnier, "A Field-Effect Transistor Based On Conjugated Alpha-Sexithienyl," *Solid State Commun.* 72, 381 (1989).
23. G. Horowitz, X. Peng, D. Fichou, and F. Garnier, "Role of Semiconductor/Insulator Interface in the Characteristics of π-Conjugated-Oligomer-Based Thin-Film Transistors," *Synth. Met.* 51, 419 (1992).
24. F. Garnier, A. Yassar, R. Hajlaoui, G. Horowitz, F. Dellofre, B. Servet, S. Ries, and P. Alnot, "Molecular Engineering of Organic Semiconductors: Design of Self-Assembly Properties in Conjugated Thiophene Oligomers," *J. Amer. Chem. Soc.* 115, 8716 (1993).
25. H. Fuchigami, A. Tsumura, and H. Koezuka, "Polythienylenevinylene Thin-Film Transistor with High Carrier Mobility," *Appl. Phys. Lett.* 63, 1372 (1993).
26. F. Garnier, R. Hajlaoui, A. Yassar, and P. Srivastava, "All-Polymer Field-Effect Transistors Realized by Printing Techniques," *Science* 265, 1684 (1994).
27. A. Dodabalapur, L. Torsi, and H. E. Katz, "Organic Transistors: Two-Dimensional Transport and Improved Electrical Characteristics," *Science* 268, 270 (1995).
28. C. D. Dimitrakopoulos, A. R. Brown, and A. Pomp, "Molecular Beam Deposited Thin Films of Pentacene for Organic Field Effect Transistor Applications," *J. Appl. Phys.* 80, 2501 (1996).
29. R. C. Haddon, A. S. Perel, R. C. Morris, T. T. M. Palstra, A. F. Hebard, and R. M. Fleming, "C_{60} Thin Film Transistors," *Appl. Phys. Lett.* 67, 121 (1995).
30. Z. Bao, A. J. Lovinger, and A. Dodabalapur, "Organic Field-Effect Transistors with High Mobility Based On Copper Phthalocyanine," *Appl. Phys. Lett.* 69, 3066 (1996).
31. Z. Bao, A. Dodabalapur, and A. J. Lovinger, "Soluble and Processable Regioregular Poly(3-hexylthiophene) for Thin Film Field-Effect Transistor Applications with High Mobility," *Appl. Phys. Lett.* 69, 4108 (1996).
32. Y.-Y. Lin, D. J. Gundlach, and T. N. Jackson, "High Mobility Pentacene Organic Thin Film Transistors," *54th Annual Device Research Conference Digest*, 1996, p. 80.
33. Y.-Y. Lin, D. J. Gundlach, S. Nelson, and T. N. Jackson, "Stacked Pentacene Layer Organic Thin-Film Transistors with Improved Characteristics," *IEEE Electron Device Lett.* 18, 606 (1997).
34. H. Sirringhaus, R. H. Friend, X. C. Li, S. C. Moratti, A. B. Holmes, and N. Feeder, "Bis(dithienothiophene) Organic Field Effect Transistors with High ON/OFF Ratio," *Appl. Phys. Lett.* 71, 3871 (1997).
35. H. Sirringhaus, N. Tessler, and R. H. Friend, "Integrated Optoelectronic Devices Based On Conjugated Polymers," *Science* 280, 1741 (1998).
36. H. E. Katz, A. J. Lovinger, and J. G. Laquindanum, "α–ω-Dihexylquaterthiophene: A Second Thin Film Single-Crystal Organic Semiconductor," *Chem. Mater.* 10, 457 (1998).
37. J. G. Laquindanum, H. E. Katz, and A. J. Lovinger, "Synthesis, Morphology, and Field-Effect Mobility of Anthradithiophenes," *J. Amer. Chem. Soc.* 120, 664 (1998).
38. H. E. Katz, A. J. Lovinger, J. Johnson, C. Kloc, T. Siergist, W. Li, Y.-Y. Lin, and A. Dodabalapur, "A Soluble and Air-Stable Organic Semiconductor with High Electron Mobility," *Nature* 404, 478 (2000).
39. J. H. Schön, S. Berg, Ch. Kloc, and B. Batlogg, "Ambipolar Pentacene Field Effect Transistors and Inverters," *Science* 287, 1022 (2000).
40. M. Pope and C. E. Swenberg, *Electronic Processes in Organic Crystals and Polymers*, 2nd Edition, Oxford University Press, New York, 1999, pp. 337–340.
41. S. F. Nelson, Y.-Y. Lin, D. J. Gundlach, and T. N. Jackson, "Temperature-Independent Transport in High-

Mobility Pentacene Transistors," *Appl. Phys. Lett.* **72**, 1854 (1998).
42. N. Karl, J. Marktanner, R. Stehle, and W. Warta, "High-Field Saturation of Charge Carrier Drift Velocities in Ultrapurified Organic Photoconductors," *Synth. Met.* **41–43**, 2473 (1991).
43. N. Karl, "Charge Carrier Mobility in Organic Molecular Crystals," *Organic Electronic Materials*, Part II, R. Farchioni and G. Grosso, Eds., Springer-Verlag, Berlin, 2000, Ch. 3.
44. W. A. Schoonveld, J. Wildeman, D. Fichou, P. A. Bobbert, B. J. Van Wees, and T. M. Klapwijk, "Coulomb-Blockade Transport in Single Crystal Organic Thin-Film Transistors," *Nature* **404**, 977 (2000).
45. C. Dimitrakopoulos, S. Purushothaman, J. Kymissis, A. Callegari, and J. M. Shaw, "Low-Voltage Organic Transistors on Plastic Comprising High-Dielectric Constant Gate Insulators," *Science* **283**, 822 (1999).
46. S. M. Sze, *Physics of Semiconductor Devices*, 2nd Edition, Wiley-Interscience Press, New York, 1981, pp. 438–453.
47. G. Horowitz, R. Hajlaoui, R. Bourgouiga, and M. Hajlaoui, "Theory of Organic Field-Effect Transistors," *Synth. Met.* **101**, 401 (1999).
48. L. Torsi, A. Dodabalapur, and H. E. Katz, "An Analytical Model for Short-Channel Organic Thin-Film Transistors," *J. Appl. Phys.* **78**, 1088 (1995).
49. Y.-Y. Lin, D. J. Gundlach, S. Nelson, and T. N. Jackson, "Pentacene-Based Organic Thin-Film Transistors," *IEEE Trans. Electron Devices* **44**, 1325 (1997).
50. J. G. Laquindanum, H. E. Katz, A. J. Lovinger, and A. Dodabalapur, "Morphological Origin of High Mobility in Pentacene Thin-Film Transistors," *Chem. Mater.* **8**, 2542 (1996).
51. C. D. Dimitrakopoulos, I. (J.) Kymissis, S. Purushothaman, D. A. Neumayer, P. R. Duncombe, and R. B. Laibowitz, "Low-Voltage, High-Mobility Pentacene Transistors with Solution-Processed High Dielectric Constant Insulators," *Adv. Mater.* **11**, 1372 (1999).
52. A. Dodabalapur, L. Torsi, and H. E. Katz, "Organic Transistors: Two-Dimensional Transport and Improved Electrical Characteristics," *Science* **268**, 270 (1995).
53. C. Py, M. D'Iorio, B. Williams, J. Fraser, M. Gao, and M. Roussy, *Abstracts of the MRS 1998 Fall Meeting*, p. 374.
54. A. Tsumura, H. Fuchigami, and H. Koezuka, "Field-Effect Transistor with a Conducting Polymer Film," *Synth. Met.* **41**, 1181 (1991).
55. J. Paloheimo, H. Stubb, P. Yli-Lahti, and P. Kuivalainen, "Field-Effect Conduction in Polyalkylthiophenes," *Synth. Met.* **41–43**, 563 (1991).
56. T.-A. Chen, X. Wu, and R. D. Rieke, "Regiocontrolled Synthesis of Poly(3-alkylthiophenes) Mediated by Rieke Zinc: Their Characterization and Solid-State Properties," *J. Amer. Chem. Soc.* **117**, 233 (1995).
57. H. Sirringhaus, P. J. Brown, R. H. Friend, M. M. Nielsen, K. Bechgaard, B. M. W. Langeveld-Voss, A. J. H. Spiering, R. A. J. Janssen, E. W. Meijer, P. T. Herwig, and D. M. de Leeuw, "Two-Dimensional Charge Transport in Self-Organized, High-Mobility Conjugated Polymers," *Nature* **401**, 685 (1999).
58. H. Sirringhaus, N. Tessler, and R. H. Friend, "Integrated, High-Mobility Polymer Field-Effect Transistors Driving Polymer Light-Emitting Diodes," *Synth. Met.* **102**, 857 (1999).
59. Z. Bao, Y. Feng, A. Dodabalapur, V. R. Raju, and A. J. Lovinger, "High-Performance Plastic Transistors Fabricated by Printing Techniques," *Chem. Mater.* **9**, 1299 (1997).
60. Z. Bao and A. J. Lovinger, "Soluble Regioregular Polythiophene Derivatives as Semiconducting Materials for Field-Effect Transistors," *Chem. Mater.* **11**, 2607 (1999).
61. J. Paloheimo, P. Kuivalainen, H. Stubb, E. Vuorimaa, and P. Yli-Lahti, "Molecular Field-Effect Transistors Using Conducting Polymer Langmuir–Blodgett Films," *Appl. Phys. Lett.* **56**, 1157 (1990).
62. J. Paloheimo, H. Stubb, P. Yli-Lahti, P. Dyreklev, and O. Inganäs, "Electronic and Optical Studies with Langmuir–Blodgett Transistors," *Thin Solid Films* **210/211**, 283 (1992).
63. G. Xu, Z. Bao, and J. T. Groves, "Langmuir–Blodgett Films of Regioregular Poly(3-hexylthiophene) as Field-Effect Transistors," *Langmuir* **16**, 1834 (2000).
64. T. Bjørnholm, D. R. Greve, N. Reitzel, T. Hassenkam, K. Kjaer, P. B. Howes, N. B. Larsen, J. Bøgelund, M. Jayaraman, P. C. Ewbank, and R. D. McCullough, "Self-Assembly of Regioregular, Amphiphilic Polythiophenes into Highly Ordered π-Stacked Conjugated Polymer Thin Films and Nanocircuits," *J. Amer. Chem. Soc.* **120**, 7643 (1998).
65. H. Akimichi, K. Waragai, S. Hotta, H. Kano, and H. Sakaki, "Field-Effect Transistors Using Alkyl Substituted Oligothiophenes," *Appl. Phys. Lett.* **58**, 1500 (1991).
66. H. E. Katz, J. G. Laquindanum, and A. J. Lovinger, "Synthesis, Solubility, and Field-Effect Mobility of Elongated and Oxa-Substituted α,ω-Dialkyl Thiophene Oligomers. Extension of 'Polar Intermediate' Synthetic Strategy and Solution Deposition on Transistor Substrates," *Chem. Mater.* **10**, 633 (1998).
67. H. E. Katz, W. Li, A. J. Lovinger, and J. G. Laquindanum, "Solution-Phase Deposition of Oligomeric TFT Semiconductors," *Synth. Met.* **102**, 897 (1999).
68. F. Garnier, R. Hajlaoui, A. E. Kassmi, G. Horowitz, L. Laigre, W. Porzio, M. Armanini, and F. Provasoli, "Dihexylquaterthiophene, a Two-Dimensional Liquid Crystal-Like Organic Semiconductor with High Transport Properties," *Chem. Mater.* **10**, 3334 (1998).
69. C. D. Dimitrakopoulos, A. Afzali-Ardakani, B. Furman, J. Kymissis, and S. Purushothaman, "*trans-trans*-2,5-Bis-[2-{5-(2,2'-bithienyl)}ethenyl]thiophene: Synthesis, Characterization, Thin Film Deposition and Fabrication of Organic Field-Effect Transistors," *Synth. Met.* **89**, 193 (1997).
70. A. R. Brown, A. Pomp, D. M. deLeeuw, D. B. M. Klaassen, E. E. Havinga, P. T. Herwig, and K. Müllen, "Precursor Route Pentacene Metal-Insulator-Semiconductor Field-Effect Transistors," *J. Appl. Phys.* **79**, 2136 (1996).
71. A. R. Brown, A. Pomp, C. M. Hart, and D. M. deLeeuw, "Logic Gates Made From Polymer Transistors and Their Use in Ring Oscillators," *Science* **270**, 972 (1995).
72. P. T. Herwig and K. Müllen, "A Soluble Pentacene Precursor: Synthesis, Solid-State Conversion into Pentacene and Application in a Field-Effect Transistor," *Adv. Mater.* **11**, 480 (1999).
73. J. H. Burroughes, R. H. Friend, and P. C. Allen, "Field-Enhanced Conductivity in Polyacetylene—Construction of a Field-Effect Transistor," *J. Phys. D: Appl. Phys.* **22**, 956 (1989).
74. C. J. Drury, C. M. J. Mutsaers, C. M. Hart, M. Matters, and D. M. deLeeuw, "Low-Cost All-Polymer Integrated Circuits," *Appl. Phys. Lett.* **73**, 108 (1998).

Received August 7, 2000; accepted for publication October 17, 2000

Christos D. Dimitrakopoulos *IBM Research Division, Thomas J. Watson Research Center, P.O. Box 218, Yorktown Heights, New York 10598 (dimitrak@us.ibm.com).* Dr. Dimitrakopoulos is currently a Research Staff Member at the IBM Thomas J. Watson Research Center, Yorktown Heights, New York, where he works on organic semiconductor devices and circuits. He has been with IBM since 1995. From 1993 to 1995 he was a postdoctoral fellow at Philips Research Laboratories in Eindhoven, The Netherlands, where he worked on organic semiconductors within the Theoretical and Experimental Physics Group. In 1993 he received his Ph.D. and M.Phil. degrees in materials science from the Graduate School of Arts and Sciences at Columbia University. He did his Ph.D. thesis research work at the IBM Thomas J. Watson Research Center. In 1989, he received his M.S. degree in materials science from the School of Engineering and Applied Science at Columbia University. He received his B.S. degree in metallurgical engineering from the National Technical University of Athens, Greece, in 1986. Dr. Dimitrakopoulos is the author of three issued patents and seven pending patents. In 2000 he received an IBM Outstanding Innovation Award and his Second Plateau Invention Achievement Award. He is a member of the Materials Research Society and a member of the Board of Directors and Treaurer of the Polymer Analysis Division, Society of Plastics Engineers.

Debra J. Mascaro *Department of Materials Science and Engineering, Massachusetts Institute of Technology, 77 Massachusetts Avenue, Cambridge, Massachusetts 02139 (dlightly@mit.edu).* Ms. Mascaro is a graduate student in the Department of Materials Science and Engineering at the Massachusetts Institute of Technology. At the time this paper was written, she was a summer intern in the Organic Electronics group at the IBM Thomas J. Watson Research Center in Yorktown Heights, New York, working with Dr. Dimitrakopoulos. She received a B.A. degree in physics from Gustavus Adolphus College in Saint Peter, Minnesota, in 1995. Her graduate research is in the area of organic field-effect transistors. Ms. Mascaro has received a National Science Foundation Fellowship and an IBM Research Fellowship.

THIS PAGE BLANK (USPTO)